

Letter

# Classification of Karst Fenglin and Fengcong Landform Units Based on Spatial Relations of Terrain Feature Points from DEMs

Xianwu Yang<sup>1,2,3,4</sup> , Guoan Tang<sup>1,3,4</sup>, Xin Meng<sup>1,3</sup> and Liyang Xiong<sup>1,3,4,\*</sup> 

<sup>1</sup> Key Laboratory of Virtual Geographic Environment (Nanjing Normal University), Ministry of Education, Nanjing 210023, China

<sup>2</sup> School of Geographic Sciences, Xinyang Normal University, Xinyang 464000, China

<sup>3</sup> School of Geography, Nanjing Normal University, Nanjing 210023, China

<sup>4</sup> Jiangsu Center for Collaborative Innovation in Geographical Information Resource Development and Application, Nanjing 210023, China

\* Correspondence: xiongliyang@njnu.edu.cn; Tel.: +86-152-5187-4227

Received: 20 June 2019; Accepted: 16 August 2019; Published: 20 August 2019



**Abstract:** In this paper, a method for extracting Fenglin and Fengcong landform units based on karst topographic feature points is proposed. First, the variable analysis window method is used to extract peaks, nadirs, and saddle points in the karst area based on digital elevation model (DEM) data. Thiessen polygons that cover the karst surface area are constructed according to the locations of the peaks and nadirs, and the attributes of the saddles are assigned to corresponding polygons. The polygons are automatically classified via grouping analysis according to the corresponding spatial combinations of peaks, saddles, and nadirs in the Fenglin and Fengcong landform units. Then, a detailed division of the surface morphology of the karst area is achieved by distinguishing various types of Fenglin or Fengcong landform units. Experiments in the Guilin research area show that the proposed method successfully distinguishes the Fenglin and Fengcong terrain areas and extracts Fengcong landform units, individual Fenglin units, and Fenglin chains. The Fengcong area covers approximately two-thirds of the whole area, the individual Fenglin area covers approximately one-fourth, and the Fenglin chain area covers approximately one-tenth. The development of Fenglin has different stages in the Guilin area. This study provides data support for the detailed morphological study of karst terrain, and proposes a new research idea for the division and extraction of karst landform units.

**Keywords:** Fenglin and Fengcong; Karst; DEM; feature points; spatial relationship; Guilin

## 1. Introduction

Fenglin and Fengcong are typical karst landforms with prominent features (Figure 1) and are among the important signs of karst landform maturity [1]. Several studies on individual morphology have been conducted in terms of karst geomorphology, and the extraction method has matured [2–10]. However, studies involving only individual morphology are insufficient. In many areas, two terrains have very similar morphologies; therefore, directly distinguishing them is difficult [11–13]. These terrains are products of various hydrological processes on carbonate rocks. Fenglin is mainly formed by runoff erosion, whereas Fengcong is mainly formed by precipitation dissolution [14–17]. Fenglin and Fengcong are products of different hydrological conditions and developmental stages [18–20]. Accurate identification of Fenglin and Fengcong topographic units is the key to understanding the karst development process [21–23].

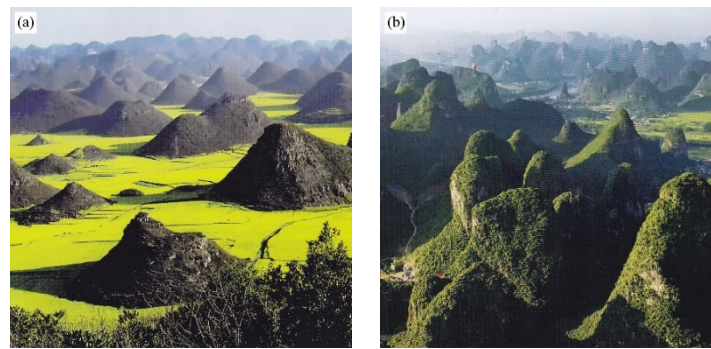


**Figure 1.** (a) Fenglin and (b) Fengcong landforms [24]. (Source: Chinese National Geography 612nd phase).

In previous studies, the distinction between Fenglin and Fengcong was made mainly according to individual morphological characteristics, such as slope, length–width ratio, and roundness. In general, most pinnacles in karst Fenglin areas are tower-shaped with large slopes and short and less dense peaks. In karst Fengcong areas, pinnacles are mostly cone-shaped, with small slopes and tall and evident saddle points [25–28]. Depressions are visible in the areas surrounded by peaks and saddles. However, no such clear differences are observed between the morphologies of Fenglin and Fengcong pinnacles. Fenglin can be conical and connected, whereas Fengcong can be tower-shaped [1,13]. The main difference between Fenglin and Fengcong is whether plains or depressions can be observed among pinnacles. In traditional karst research, single pinnacles are typically regarded as Fenglin, whereas pinnacle chains are regarded as Fengcong. However, Fenglin pinnacles can also be connected, and individual pinnacles can be surrounded by Fengcong. At present, research on the extraction of pinnacle chains in Fenglin plain areas remains scarce, and studies on Fenglin and Fengcong mixed areas are rare [29]. Thus, the results of Fenglin and Fengcong topographic studies based on digital elevation models (DEMs) frequently deviate from the actual situation.

To date, two main methods are used to extract Fenglin and Fengcong landform units based on DEM. One method is based on the extraction of feature lines [24,29]. The common idea is to identify mutation lines, such as contours and toe lines, by extracting the catastrophe or extremum of the terrain based on DEMs. The mutation lines are only the numerical calculations of gray values, and geographic characteristics are not considered. The accuracy of the extraction results is only a line with abrupt topographic change, which is insufficient for identifying whether the area is Fenglin or Fengcong. Individual landform units can be extracted on the basis of the nested structure of contours, but such a method wrongly regards the connected Fenglin pinnacles as Fengcong in most cases. The second method involves constructing a recognition model of Fenglin, Fengcong, and other karst landform units and extracting object-oriented texture features according to the morphological characteristics of objects [30–34]. This method mainly calculates the objects in the analysis windows by terrain factors, such as elevation, slope, curvature, and texture, then it differentiates karst landform types. This method considers the entire topographic unities in a region. However, the structure of karst topography is typically complex and frequently includes various topographic units (e.g., mixed zones of Fenglin, Fengcong, and depressions). No unified form exists for various landform units (Fenglin pinnacles can be cone-shaped or clustered, and slope largely varies across areas). However, there may be no significant differences in morphology between Fenglin and Fengcong pinnacles. This method cannot extract individual landform units in mixed areas, and these units are frequently treated as a whole.

Peaks, saddles, and nadirs are the typical feature points of Fenglin and Fengcong karst geomorphology. Peaks correspond to pinnacles, whereas nadirs correspond to depressions. These feature points and their spatial relations reflect different karst topographic units, which can reflect the development process of karst landforms. Accurately extracting peaks, saddles, and nadirs through traditional methods is difficult due to the complex topography of karst areas. Studies that focus

on feature point extraction in Fenglin and Fengcong areas are scarce and do not focus on karst spatial relations based on these feature points [35–37]. In previous studies [13,19,29], Fenglin chains were always regarded as Fengcong terrain. Moreover, Fenglin chains are an important sign of karst development. Therefore, in this study, karst landform units are classified into three types: Fengcong, typical Fenglin, and Fenglin chains. Here, Fenglin chains are units composed of pinnacle chains, which are several striped pinnacles with a common base.

This paper proposes a novel approach for distinguishing surface karst topography; that is, distinguishing between Fenglin and Fengcong topography based on the spatial relationship of peaks, saddles, and nadirs in the karst area without considering the morphological characteristics of single pinnacles. If obvious saddles exist among pinnacles, and these saddles can form closed areas around a circle with depressions in the middle, then these pinnacles are Fengcong areas. If a single individual pinnacle exists without saddles, then it is a typical Fenglin area. If saddles exist among pinnacles but they cannot form closed areas, and no depression exists, then these pinnacles are Fenglin chains. In this study, Guilin, China, was taken as the study area. Fengcong landform units, individual Fenglin units, and Fenglin chains were extracted. This research lays a foundation for the accurate study of karst surface morphology.

## 2. Study Area and Data

Guilin (110.33°–110.45° E, 24.90°–25.10° N) is recognized as the most typical and obvious karst area in the world. It is the main area where Fenglin and Fengcong coexist and is regarded as one of the most beautiful and spectacular landform assemblages in China, and in the world [38,39]. The main study area (Figure 2) is located in Guilin, Guangxi Province, southwest China, has a total area of 236 km<sup>2</sup>, and is mainly composed of the Rongxian Formation of the Upper Devonian. Its elevation is high in the east and low in the west and mainly consists of middle and low mountain areas. In general, the pinnacles are cone-shaped, with a height of approximately 200 m. The Fengcong depression area is dominant in the east, whereas the Fenglin plain area is dominant in the west.

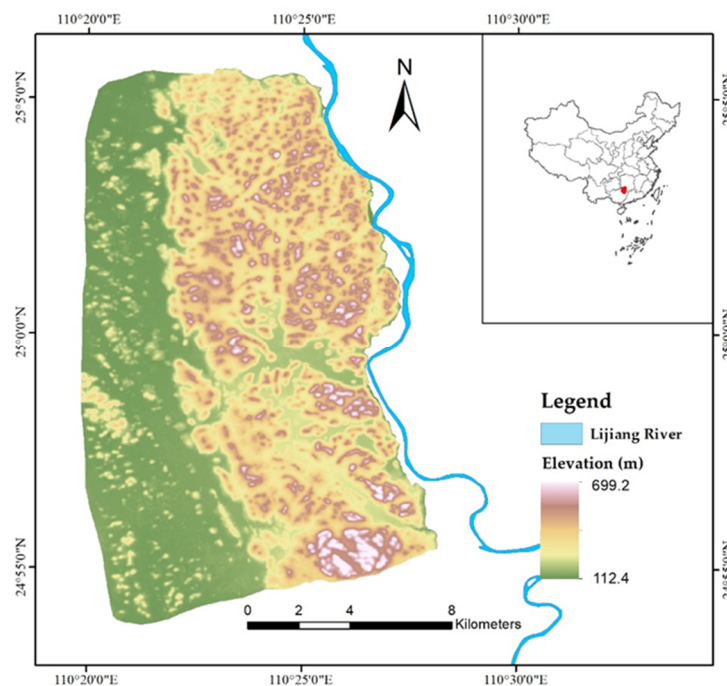


**Figure 2.** Study area in Guilin, Guangxi Province, China.

Individual Fenglin pinnacles are located at the edge of Fengcong, and isolated Fengcong is located in the Fenglin plain area. In the middle, a valley lies along the east–west direction. The study area

features a subtropical monsoon climate, and precipitation decreases from northwest to southeast. Small surface runoffs are visible in the west, and underground rivers can be found in the east. It is a complete hydrogeological unit [40–42].

The test data are DEMs with 5 m grid size interpolated from the contours of 1:10,000 topographic maps with a 5 m contour interval produced by the National Administration of Surveying, Mapping and Geoinformation of China. The spatial resolution of the data is 5 m, and the vertical accuracy is 1.2 m [43].

### 3. Methods

In karst geomorphology, a typical Fengcong area towers above the surrounding terrain, and its boundary is either adjacent to the plain or surrounded by rivers with little external water involved in development. Isolated Fengcong is mainly distributed in the Fenglin plain with low height and small enclosed depressions. The typical Fenglin plain is mostly composed of single pinnacles with steep slopes and has low height. A Fenglin chain appears on small flat ground among Fengcong and is similar to a single Fenglin in height. The main difference between Fenglin and Fengcong is the presence or absence of depressions or plains among pinnacles.

In this study, topographic feature points such as peaks, saddles, and nadirs are extracted on the basis of DEM data. Then, spatial relation models of typical Fenglin and Fengcong terrain are constructed according to their morphological characteristics. Different landform units are automatically extracted according to their spatial relations.

#### 3.1. Extraction of Feature Points

In a karst area, peaks and nadirs correspond to the highest and lowest points of pinnacles and depressions, respectively, whereas saddles are the intersection points of valley and ridge lines. Extracting peaks and nadirs in a karst area involves identifying the extreme points of a region. This study proposes an extraction method for Fenglin and Fengcong peaks and nadirs based on variably sized windows, which are the key contours in the study area. The contours that represent the boundaries of Fenglin and Fengcong basic landform units are defined as the key contours. Key contour nodes are selected from the contour tree based on the inclusion relationship of nodes. The maximum closed contour line that includes only a single contour is taken as the key contour line and extracted. The hierarchical structure of the contour lines is established, and the key contour lines are selected by the methods proposed by Liang and Wu (as shown in Figure 3a) [29,44]. In traditional methods, the analysis window is often used to calculate the extremum points in each contour circle [45–48]. However, traditional methods based on fixed window analysis are not always applicable in this study area. When the analysis window is small, numerous extreme points will be found in a large area. When the analysis window is extremely large, several small mountains are regarded as a single unit, and several key points are omitted. Thus, extraction results are often inaccurate.

In this study, the size of the analysis window is set in accordance with the area surrounded by the key contours. The minimum key contour range is used as the size of the analysis window to search the extremum point. When only one extremum in the contour area is enclosed by each key contour line, the point is recorded, and the contour area is deleted. That is, each key contour corresponds to an analysis window of the same size, and only one extremum point can be found in such a window. Then, the analysis window for the remaining areas is expanded and operated in a loop until only one extremum point can be found in each key contour area. When the contour is located in a positive terrain, the maximum point is a peak. If the contour coil is located in a negative terrain, then the limit point is a nadir. The main workflow is shown in Figure 3b.

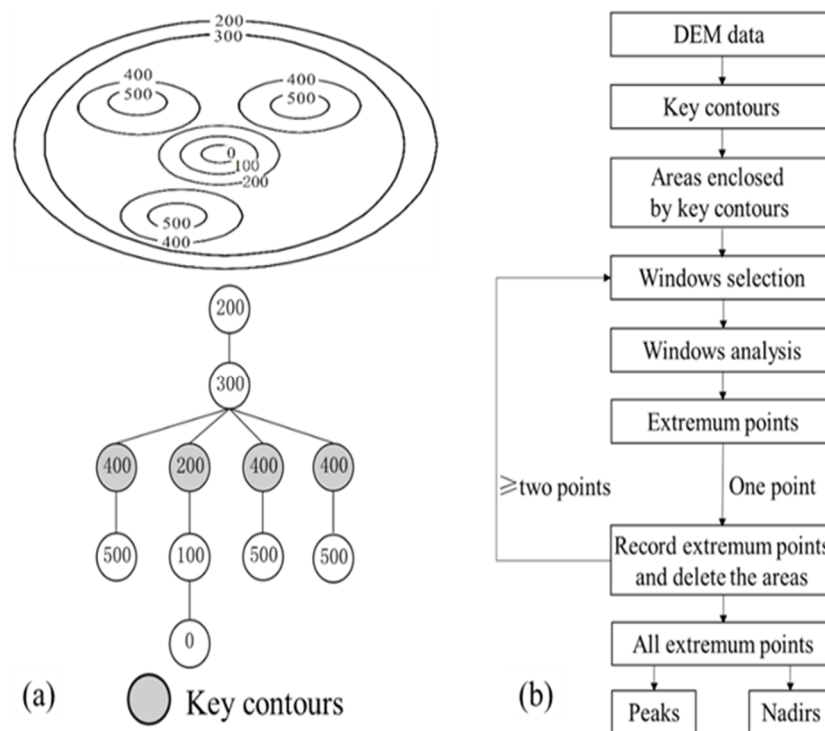


**Figure 3.** (a) Typical karst landform and contour structure; (b) flowchart of the methodology.

Saddles in the karst area can be seen as intersections of ridge and valley lines [49–51]. The ridge and valley lines are usually extracted from DEM data using the digital terrain analysis method. In this study, the commonly used confluence accumulation method is utilized to extract the ridge and valley lines [52–55]. The saddles are located at the intersections of ridge and valley lines; however, not all intersections are saddles due to the influence of surface uplift. Real saddles can be extracted from intersection points based on the characteristics of small slope and large slope changing the rate of saddles in a karst terrain [56].

### 3.2. Constructing Spatial Relationship between Feature Points

The spatial relationship among feature points is constructed according to the distribution of peaks, saddles, and nadirs in Fenglin and Fengcong terrains. In Fenglin, the typical cases are single individual pinnacles (A in Figure 4). These pinnacles only include peaks with no obvious saddles or nadirs around them. The peaks and control areas of these pinnacles can be easily found, and the single Fenglin terrain unit can be extracted. Moreover, pinnacle chains (B in Figure 4) are observed in addition to individual pinnacles. For such topographic units, peaks and saddles are distributed in a linear manner. Peaks and saddles cannot form a closed area, and no nadir is observed in the middle. In Fengcong, peaks and saddles tend to form a closed polygon with typical nadirs in the middle (C in Figure 4). A typical Fengcong terrain unit is composed of a nadir in the center, surrounded by peaks and saddles. This type of terrain is identified by establishing spatial relationships among peaks, saddles, and nadirs. First, the nadir locations in the study area are extracted. Then, each nadir is taken as a center to search the peaks and saddles that are nearest to it. An area that is composed of these peaks and saddles is a typical Fengcong unit.

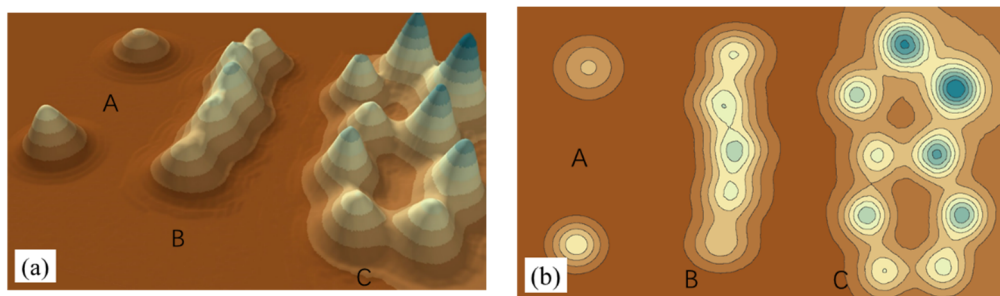


**Figure 4.** Typical Fenglin and Fengcong landform units. (a) 3D view of karst landform units; (b) 2D view of karst landform units (A: individual Fenglin B: Fenglin chain C: typical Fengcong).

According to the morphological characteristics and spatial combinations of the Fenglin and Fengcong topography, we found that peaks and nadirs are the main control points of the entire study area. Peaks, saddles, and nadirs construct a system of karst feature points. Peaks control the positive terrain, whereas nadirs control the negative terrain. In this study, peaks and nadirs are combined as seed points to create the Thiessen polygons. Therefore, the control area of the positive and negative terrains is obtained through the Thiessen polygons. By relating the attribute information of extracted peaks, saddles, and nadirs to corresponding Thiessen polygons, the spatial relationships of peaks, saddles, and nadirs are expressed in the form of polygon adjacency.

### 3.3. Division of Fenglin and Fengcong Landform Units

By analyzing the spatial relationship of feature points, the study area can be divided into three types of units: Fengcong, Fenglin, and Fenglin chains. The discriminant rules are as follows:

- (1) Nadirs are present in the Fengcong units, and peaks and saddles are distributed around the nadirs.
- (2) The typical Fenglin unit is composed of individual pinnacles (peaks), and no saddles or nadirs are present around the pinnacles. The nearest point is also a peak.
- (3) The Fenglin with pinnacle chains is typically distributed in strips; peaks and saddles are distributed alternately, whereas strips are open.

According to these rules, the corresponding polygons are divided into three groups: Fengcong units, typical Fenglin units, and pinnacle chain units.

Polygons with attributes of various feature points are classified via grouping analysis, which uses unsupervised machine learning to determine the natural grouping of data [57,58]. This research mainly uses the ArcGIS platform. This method groups elements according to attributes and optional spatial or temporal constraints. Element similarity is based on a set of characteristics specified by the analysis field parameters. It can also include spatial or spatiotemporal attributes. When spatial or spatiotemporal constraints are specified, the algorithm will use a connected graph (minimum span tree) to seek natural groupings.

First, we start with polygons that contain nadirs (polygon A in Figure 5) and search the polygons adjacent to them. These polygons belong to the Fengcong area. In these circles of polygons, if peaks and saddles are present in the polygon (polygon B in Figure 5), then the search for an adjacent polygon is continued (polygon C in Figure 5) in the direction of the peaks–saddles, which also belong to the Fengcong area. Then, we start with the polygon that contains peaks only (polygon E in Figure 5) and search for adjacent polygons. If all the surrounding polygons contain peaks only, then they belong to an individual Fenglin area. In the remaining polygons, start with the polygons that contain peaks and saddles at the same time, take them as seed points, and search the polygons along the direction from peak to saddle. If the polygon belongs to the Fengcong area, then the seed point also belongs to the Fengcong area (polygon D in Figure 5). If the polygon is unlabeled, then the two polygons form a pinnacle chain (polygons F and G in Figure 5). Finally, the remaining unmarked polygons belong to

individual Fenglin. The boundaries of Thiessen polygons do not exactly coincide with actual Fenglin or Fengcong units. However, for the entire study area, the control area of Thiessen polygons is roughly consistent with the actual Fenglin or Fengcong area. Therefore, the range of Fenglin or Fengcong landform units can be represented by the range of Thiessen polygons.

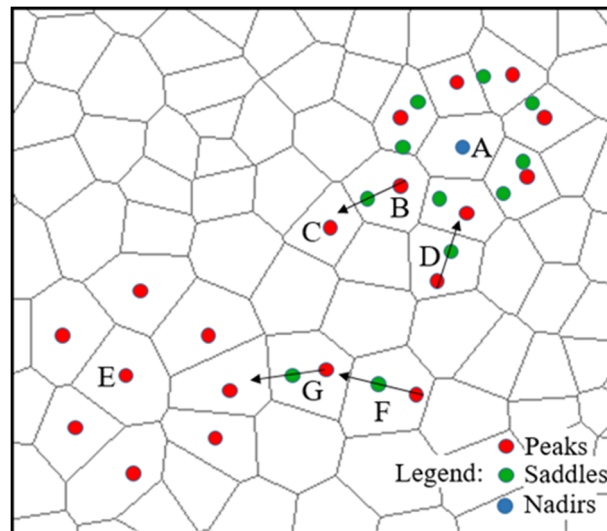


Figure 5. Process of grouping analysis method.

## 4. Results

### 4.1. Extraction of Peaks, Saddles, and Nadirs

The contour lines are generated with a contour distance of 10 m from the 5 m resolution DEM data in the Guilin area. We establish the hierarchical structure of the contour lines and select the key contour lines (as shown in Figure 6a). The maximum point is the peak of the region, whereas the minimum point is the nadir point. Then, the saddles in this area are calculated by the changing rate of slope method (Figure 6b). A total of 1061 peaks, 958 saddles, and 252 nadirs are extracted in this area (Figure 6c).

In terms of the spatial locations of the extracted feature points, peaks are uniformly distributed in the entire region. The density of the peaks in the western part of the study area is slightly low. Saddles are mainly distributed along the eastern Lijiang River, scattered in the west, and mostly concentrated in the northeast. The nadirs are only distributed along the Lijiang River. The north is denser than the south, and sporadic nadirs are present in the middle of the east. According to the distribution of these characteristic points, the study area can be divided into eastern and western parts. In the western part, the terrain is flat with very little fluctuation. Pinnacles are scattered sparsely on a large area of flat land with a large amount of external water entering the area. The eastern part is generally Fengcong. The northeastern part is a complete Fengcong area with a uniform interior and nearly flattened pinnacle tops. In this area, pinnacles are distributed in large or massive clusters with many closed and infiltrative negative morphologies, such as sinkholes, dolines, and nadirs. In the eastern middle part of the study area, groundwater activity is significant, surface and underground karst development is strong, land surface is incised fiercely, the fluctuation between peaks is high, and small plain areas are present. The southeastern part of the study area is composed of relatively complete carbonate rock with a low degree of dissolution and poor development. Pinnacles are not obviously differentiated. In addition, the saddles have relatively high elevation.

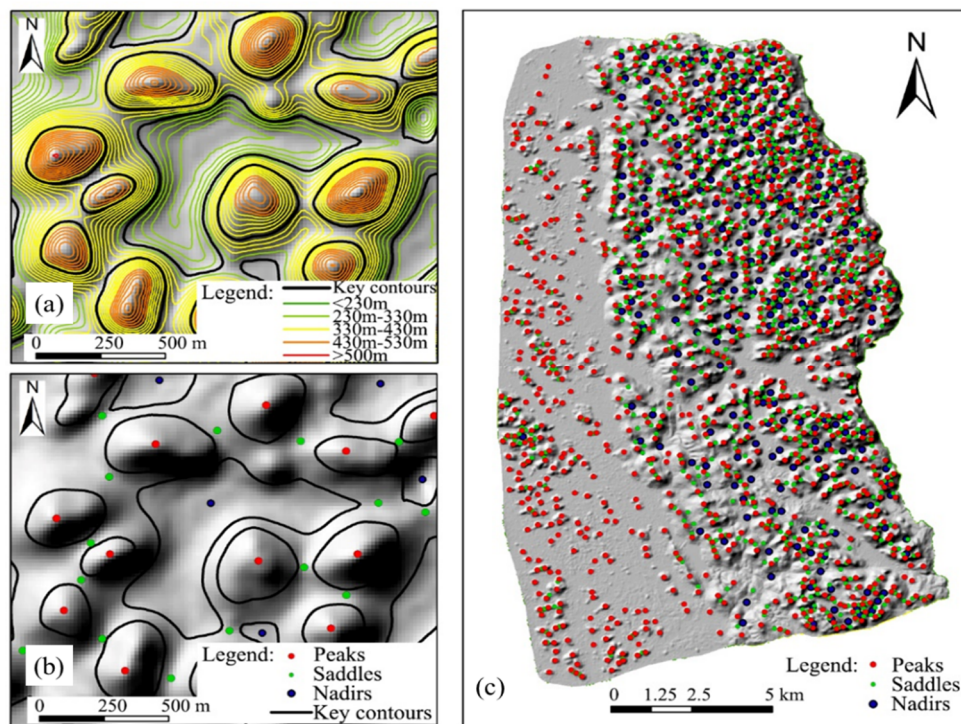


**Figure 6.** Extraction of peaks, saddles, and nadirs (a) key contour (b) feature points (c) final extraction results.

#### 4.2. Fenglin and Fengcong

A total of 1312 Thiessen polygons are found in the study area. The largest and smallest areas are 1.21 and 0.028 km<sup>2</sup>, respectively. The average area is 0.18 km<sup>2</sup>. The attribute information of peaks, saddles, and nadirs is related to the corresponding polygons. Through the grouping analysis method, the polygons are divided into three groups according to the spatial relations of peaks, saddles, and nadirs in Fengcong, typical Fenglin, and Fenglin chains (Figure 7). A total of 1043 Fengcong units are present, with an area of 155.9 km<sup>2</sup>, which accounts for 66% of the total study area (including 25 isolated Fengcong units, with an area of 3.77 km<sup>2</sup>). Specifically, 173 individual Fenglin and 96 Fenglin chains are identified with areas of 58.7 and 21.3 km<sup>2</sup>, accounting for 25% and 9% of the total study area, respectively. Table 1 provides the elevation of peaks and saddles across parts. From the distribution of Fenglin and Fengcong, two Fengcong areas are identified. The main part is distributed along the bank of the Lijiang River with a small Fenglin area in the middle, which consists of a Fenglin pinnacle chain with five peaks and seven individual Fenglin units. Another Fengcong area is located at the edge of the Fenglin area in the western part, where Fenglin chains and individual Fenglin pinnacles coexist.

Statistical analysis was conducted based on the data of characteristic points that correspond to individual Fenglin, chain Fenglin, and Fengcong areas (Table 1).

According to the statistical analysis of elevation, the average elevation of saddles in Fenglin area is 234.3 m. The number of saddles below 235 m is 46, which accounts for 75.4% of the total Fenglin area. Four saddles above 300 m are distributed in the Fengcong enclosure area on the right bank of the Lijiang River. The average elevation of saddles in the Fengcong area is 379.3 m. A total of 761 saddles above 300 m are identified, accounting for 84.8% of the total Fengcong area. Findings show that significant differences exist in the elevation of saddles between the Fengcong and Fenglin areas (Figure 8).

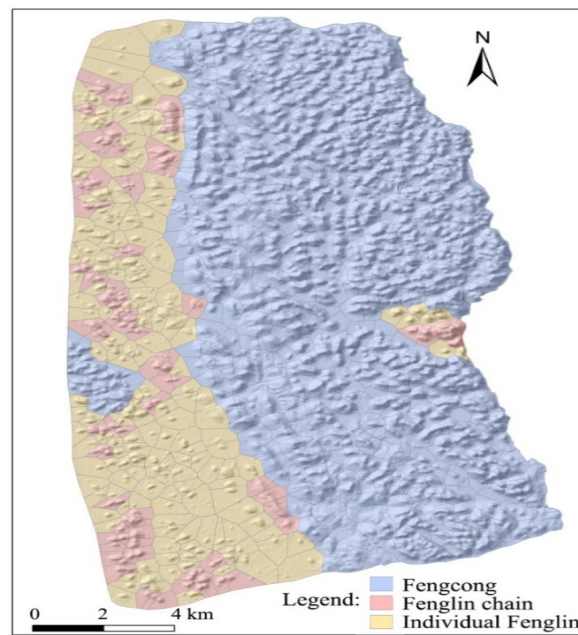


Figure 7. Distribution of Fenglin and Fengcong in the study area.

Table 1. Statistics on the number and elevation of extracted feature points.

| Name                   | Peaks          |                  |                     | Saddles          |                       | Nadirs |
|------------------------|----------------|------------------|---------------------|------------------|-----------------------|--------|
|                        | Fengcong Peaks | Individual Peaks | Fenglin Chain Peaks | Fengcong Saddles | Fenglin Chain Saddles |        |
| Total                  | 792            | 173              | 96                  | 897              | 61                    | 252    |
| Maximum elevation (m)  | 699.2          | 414.9            | 569.5               | 628.1            | 510.4                 | 588.8  |
| Minimum elevation (m)  | 221.3          | 195.6            | 210.2               | 166.8            | 195.1                 | 155.4  |
| Average elevation (m)  | 466.9          | 241.3            | 273.9               | 379.3            | 234.3                 | 311.9  |
| Median elevation (m)   | 472.6          | 233.3            | 265.6               | 376.5            | 217.9                 | 299.1  |
| Standard deviation (m) | 86.1           | 36.1             | 56.5                | 78.4             | 47.7                  | 71.6   |

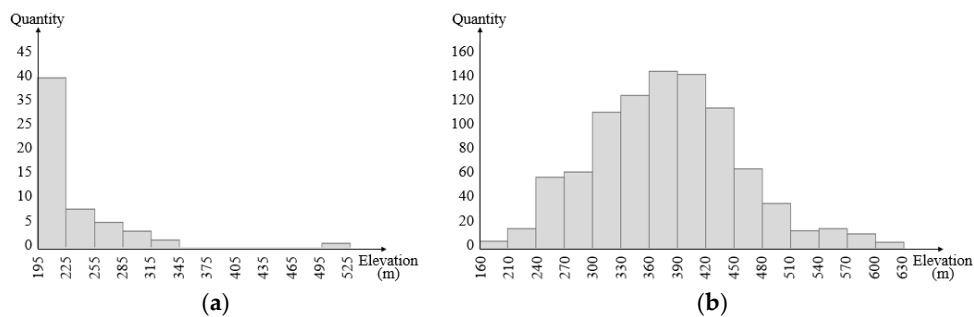
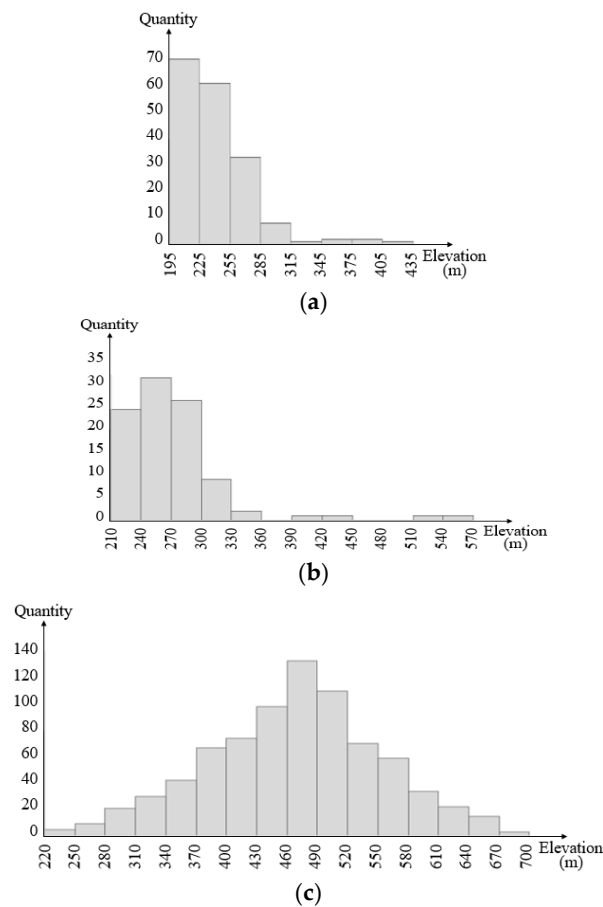


Figure 8. Statistical chart of saddle elevation. (a) Fenglin; (b) Fengcong.

The elevation of peaks in the Fenglin area is concentrated in the low-value area, and the distribution in the Fengcong area is similar to the normal distribution. The average elevation of peaks in the individual Fenglin area is 241.3 m, and 90% of the peaks are distributed below 270 m. The average elevation of peaks in the chain Fenglin area is 273.9 m; 81 peaks are distributed below 300 m, accounting for 84.4% of the total Fenglin peaks. The average elevation of peaks in the Fengcong area is 466.9 m, and 750 peaks are distributed above 320 m, accounting for 94.7% of the total Fengcong peaks. Findings show that among the Fengcong, Fenglin chain, and individual Fenglin areas, the elevation difference of peaks is also evident (Figure 9).



**Figure 9.** Statistical chart of peak elevation. (a) Individual Fenglin; (b) Fenglin chain; (c) Fengcong.

## 5. Discussion

### 5.1. Comparison with Other Methods Used in the Guilin Area

Guilin is a typical area, where karst Fenglin and Fengcong coexist. Different methods were proposed in previous research to extract topographic units in this area. In the Guilin area, Meng [24] used terrain openness to extract Fenglin and Fengcong, and Liang [29] used the contour tree method. Although they extracted the terrain boundary, they regarded individual pinnacles as Fenglin and mistook the Fenglin chains as Fengcong (Figure 10). This finding is inconsistent with reality. The present study uses the traditional method to extract the boundaries of landform units. By combining the results of Thiessen polygon grouping, the correct classification of each terrain unit can be obtained. The blue wireframe regions in the Yangdi and Dabu areas of Guilin were marked as Fengcong by previous methods. In the present study, they are regarded as Fenglin chains. Most of the banks of the Lijiang River in Guilin is Fengcong terrain. However, it is in the middle of two large Fengcong terrains in the Yangdi area with small valleys formed by surface water alluviation (Figure 10a). A small Fenglin plain terrain is formed in this area due to the effect of surface water. Furthermore, six distinct individual pinnacles are observed in the plain. A group of pinnacles near the bank of the Lijiang River is noted. The areas surrounded by pinnacles are observed as being positive areas. Obvious ridges and saddles are present, but nadirs are lacking among the pinnacles. Surface precipitation flows along the ridges to the flat land around the pinnacles and then into the Lijiang River. In other words, generating nadirs in this area is impossible, to the extent that it cannot be identified as a Fengcong area. Similarly, Dabu in Guilin is generally a Fenglin plain (Figure 10b). Several pinnacles are connected on the plain. Pinnacles cannot form in a closed area, and no depression exists in the middle. The pinnacle group is also a Fenglin unit.

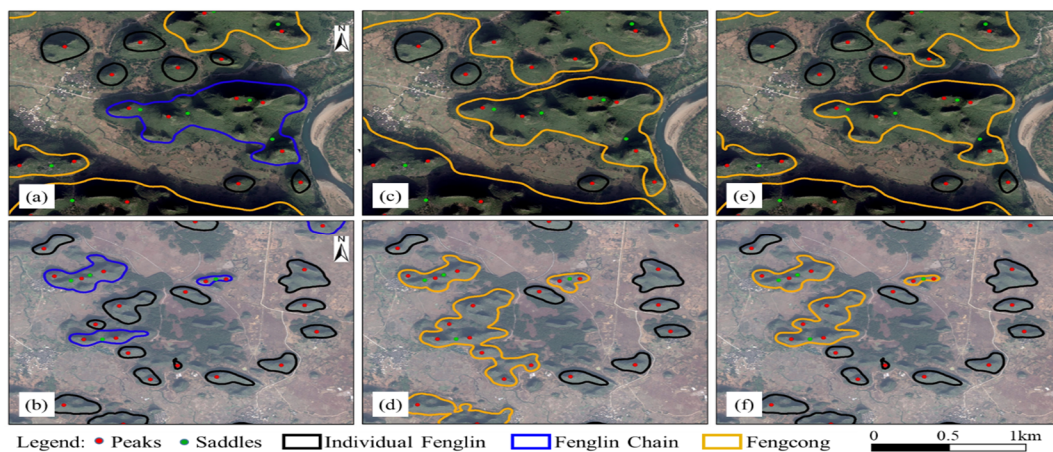


**Figure 10.** Comparison with existing methods: (a,b) results of feature point method; (c,d) results of Liang et al. [29]; (e,f) results of Meng et al. [24]. (a,c,e) In the Yangdi area of Guilin, Fenglin chains surrounded by Fengcong. (b,d,f) In the Dabu area of Guilin, Fenglin chains surrounded by individual Fenglin.

Existing methods for distinguishing Fenglin and Fengcong terrain are based on the morphological characteristics of pinnacles and whether the pinnacles are connected. However, the main difference between Fenglin and Fengcong terrains is whether it is a plain or a depression that is distributed among pinnacles. If no obvious depression is noted among connected pinnacles, then precipitation cannot form a convergence. Thus, dissolving into a depression is difficult; therefore, the terrain can only be considered to be a Fenglin area.

## 5.2. Implication of Landform Development

Typical Fengcong and Fenglin areas are clear signs of a karst geomorphological development stage. Fenglin chain is an intermediate process from Fengcong to Fenglin [1,13,14,59,60]. The geomorphic development stage of this area can be inferred according to the distribution of Fenglin and Fengcong topography in different areas. The distribution of peaks varies greatly in different areas. From the results of Fenglin and Fengcong extraction, two forms of Fengcong are found in Guilin. The typical Fengcong area in the east rises above the surrounding terrain with the Lijiang River in the east and the plain terrain in the west. Almost no exogenous water is involved in this development. In the western part of Bao'an, a region of isolated Fengcong units scattered over the Fenglin plain, is observed. The typical Fenglin area is located on the plain with individual pinnacles as the main part and a plain among pinnacles. In several areas, several pinnacle bases are connected to form a Fenglin chain. These pinnacles are typically distributed along a line. Saddles are observed, but no closed depression exists in the middle of the pinnacles. Additional statistics show that the vast majority of the Fenglin chains include two pinnacles. In the study area, six Fenglin chains have three pinnacles, five Fenglin chains have four pinnacles, and only two Fenglin chains have five pinnacles.

In the development of karst geomorphology, Fengcong areas are mainly affected by precipitation erosion, which forms depressions, and underground rivers in the interior. With the enhancement of dissolution, areas of depression increase gradually; the depth increases and the pinnacles shrink inward. When precipitation is high, the underground drainage system cannot discharge surface water in time. Thus, temporary drainage channels will form on the ground surface. Surface water will wash the Fengcong topography along the river. Over time, gullies will form in the Fengcong area, small alluvial plains will form near rivers, and a small Fenglin area will form in the Fengcong area. Fenglin landforms are mainly eroded by exogenous water. When Fenglin landform begins to develop, the flow to the low level of the terrain is large. However, the flow route is random. Exogenous water divides the surface into small isolated karst units. Influenced by varying precipitation and water erosion, the sizes

of the isolated karst units divided by water channels are different, and the rock mass is distributed in strips along the direction of the water flow. Small karst rocks gradually develop into individual Fenglin units. The dissolution of precipitation in large karst units is also synchronized, thereby forming small depressions or sinkholes. Flow water mainly occurs in the edge area, which forms isolated Fengcong units. The Fenglin terrain is considered an important sign of karst maturity. Fenglin units in the Fengcong area indicate that phased surface rivers are present and karst has developed to maturity. If Fenglin chains or isolated Fengcong are present in the Fenglin plain, then the karst in the area is continuously developing.

## 6. Conclusions

Fenglin and Fengcong terrains are extracted based on the spatial relationships of karst feature points. We base our analysis on the connotation of Fengcong and Fenglin topographic concepts in karst areas. We consider that the key to distinguishing Fenglin from Fengcong is whether a closed area is present in the middle of the pinnacles. Peaks, saddles, and nadirs are extracted by using DEM data and the digital terrain analysis method. Thiessen polygons are constructed in accordance with the conclusion that peaks and nadirs are the main control points of positive and negative terrains. Combined with the spatial relationship of the three feature points, the study area is divided by the grouping analysis method into three categories: Fengcong, typical Fenglin, and Fenglin chain areas. By analyzing the spatial distributions and morphological characteristics of Fenglin topography, we find that the development of Fenglin has different stages in the Guilin area. The central part of the Fengcong area may possibly develop into Fenglin. This method provides a scientific basis for the quantitative analysis of Fenglin and Fengcong morphological characteristics of karst in the future. Furthermore, this method provides a new concept for karst research. This method is more automated than the previous manual survey and interpretation of remote sensing images and thus is especially suitable for the extraction of Fenglin and Fengcong in complex mixed areas.

However, the extraction of feature points in complex areas of karst terrain is insufficiently accurate because of the limitations of data quality and the analysis method. Different peaks may be obtained by selecting different contour distances during the extraction of feature points. This variation in peaks may have certain effects on the results of subsequent analysis. In the Fengcong area, some small terrain boundaries are difficult to present accurately. In addition, the proposed method has been successfully used in the karst landform area of Guilin. However, different karst areas have their own specific karst morphology with highly complicated landform units. Especially at the microscale, many small karst landform units should be considered for a good understanding of the karst landform evolution process. These issues should be solved in future research.

**Author Contributions:** X.Y. proposed the method, performed analysis and wrote the paper. L.X. conceived the study, designed the experiments. X.M. collected and processed the data. G.T. conceptualization, and review & editing of this paper.

**Funding:** This research has been supported by the National Natural Science Foundation of China (No. 41930102, No. 41701449, No. 41971333, and No. 41671389), Key Research Projects of Henan Higher Education Institutions (16A170015), Nanhu Scholars Program for Young Scholars of XYNU.

**Acknowledgments:** We are grateful to the members of the DEM research group for their stirring discussions and the reviewers for their helpful comments on this manuscript. We would like to thank Wen Dai, Hu Ding, Ziyang Dai, Jingwei Li and Xue Yang for their help in data pro-processing and paper revision.

**Conflicts of Interest:** The authors declare no conflict of interest.

## References

1. Zhu, X. Discussions on fenglin karst in China. *Carsologica Sin.* **2009**, *28*, 155–168.
2. Brook, G.A.; Hanson, M. Double Fourier series analysis of cockpit and doline karst near Browns Town, Jamaica. *Phys. Geogr.* **1991**, *12*, 37–54. [[CrossRef](#)]

3. Day, M.J.; Chenoweth, M.S. The karstlands of Trinidad and Tobago, their land use and conservation. *Geogr. J.* **2004**, *170*, 256–266. [[CrossRef](#)]
4. Obu, J.; Podobnikar, T. Algorithm for karst depression recognition using digital terrain models. *Géod. Vestn.* **2013**, *57*, 260–270. [[CrossRef](#)]
5. Čeru, T.; Šegina, E.; Gosar, A. Geomorphological Dating of Pleistocene Conglomerates in Central Slovenia Based on Spatial Analyses of Dolines Using LiDAR and Ground Penetrating Radar. *Remote Sens.* **2017**, *9*, 1213. [[CrossRef](#)]
6. Šegina, E.; Benac, Č.; Rubinić, J.; Knez, M. Morphometric analyses of dolines—The problem of delineation and calculation of basic parameters. *Acta Carsologica* **2018**, *47*, 23–33. [[CrossRef](#)]
7. Hofierka, J.; Gallay, M.; Bandura, P.; Šašak, J. Identification of karst sinkholes in a forested karst landscape using airborne laser scanning data and water flow analysis. *Geomorphology* **2018**, *308*, 265–277. [[CrossRef](#)]
8. Zumpano, V.; Pisano, L.; Parise, M. An integrated framework to identify and analyze karst sinkholes. *Geomorphology* **2019**, *332*, 213–225. [[CrossRef](#)]
9. Moreno-Gómez, M.; Liedl, R.; Stefan, C. A New GIS-Based Model for Karst Dolines Mapping Using LiDAR; Application of a Multidepth Threshold Approach in the Yucatan Karst, Mexico. *Remote Sens.* **2019**, *11*, 1147.
10. Kim, Y.J.; Nam, B.H.; Youn, H. Sinkhole Detection and Characterization Using LiDAR-Derived DEM with Logistic Regression. *Remote Sens.* **2019**, *11*, 1592. [[CrossRef](#)]
11. Zhu, D. Evolution of peak cluster-depression in Guilin area and morphometric measurement. *Carsologica Sin.* **1982**, *2*, 127–134.
12. Yang, M.; Zhang, Y.; Smart, P.; Waltham, T. Karst geomorphology of western Guizhou, China. *Carsologica Sin.* **1987**, *6*, 345–352.
13. Waltham, T. Fengcong, fenglin, cone karst and tower karst. *Cave Karst Sci.* **2008**, *35*, 77–88.
14. Day, M.J. The role of valley systems in the evolution of tropical karstlands. In *Evolution of Karst: From Prekarst to Cessation*; Gabrovsek, F., Ed.; Zalozba ZRC: Ljubljana, Slovenia, 2002; pp. 235–241.
15. Zhou, C. *A Dictionary of Geomorphology*; China Water Power Press: Beijing, China, 2006.
16. Tüfekçi, K.; Sener, M. Evaluating of karstification in the Menteşe Region of southwest Turkey with GIS and remote sensing applications. *Z. für Geomorphol.* **2007**, *51*, 45–61.
17. Yuan, D. *Modern karstification*; Science Press: Beijing, China, 2016.
18. Yang, M.; He, C. Developmental Characteristics of Cone-shaped Karst in China. In *Proceedings of Danxia Mountain*; Science Press: Beijing, China, 2004.
19. Hill, C.A.; Eberz, N.; Buecher, R.H. A Karst Connection model for Grand Canyon, Arizona, USA. *Geomorphology* **2008**, *95*, 316–334. [[CrossRef](#)]
20. Wang, D.; Xu, M.; Qi, J.; Zang, Q. Analysis on morphologic features of the peak-cluster depression in Qiubei, Southeast Yunnan. *Carsologica Sin.* **2010**, *29*, 239–245.
21. Smith, D.I. Process, Land-forms and Climate in Limestone Regions. In *Geomorphology and Climate*; Wiley: London, UK, 1976.
22. Yang, M.; Liang, H. The processes of evolution dynamic of cone karst and the exploitation of the water resource. *Carsologica Sin.* **2000**, *1*, 44–51.
23. Thrailkill, J. *Karst Geomorphology and Hydrology; Geomorphology and Hydrology of Karst Terrains*; Wiley: Hoboken, NJ, USA, 2007.
24. Meng, X.; Xiong, L.-Y.; Yang, X.-W.; Yang, B.-S.; Tang, G.-A. A terrain openness index for the extraction of karst Fenglin and Fengcong landform units from DEMs. *J. Mt. Sci.* **2018**, *15*, 752–764. [[CrossRef](#)]
25. Yuan, D. About Fenglin karst. *Geol. Guangxi* **1984**, *1*, 79–84.
26. Dian, Z. A morphological analysis of Tibetan limestone pinnacles: Are they remnants of tropical karst towers and cones? *Geomorphology* **1996**, *15*, 79–91. [[CrossRef](#)]
27. Tang, T.; Day, M.J. Field survey and analysis of hillslopes on tower karst in Guilin, southern China. *Earth Surf. Process. Landf.* **2000**, *25*, 1221–1235. [[CrossRef](#)]
28. Yue, Y.; Zhang, B.; Wang, K.; Liu, B.; Li, R.; Jiao, Q.; Yang, Q.; Zhang, M. Spectral indices for estimating ecological indicators of karst rocky desertification. *Int. J. Remote Sens.* **2010**, *31*, 2115–2122. [[CrossRef](#)]
29. Liang, F.; Du, Y.; Ge, Y.; Li, C. A quantitative morphometric comparison of cockpit and doline karst landforms. *J. Geogr. Sci.* **2014**, *24*, 1069–1082. [[CrossRef](#)]
30. Viles, H.A.; Tucker, G.E.; Lyew-Ayee, P.; Viles, H.; Tucker, G.; Lyew-Ayee, P. The use of GIS-based digital morphometric techniques in the study of cockpit karst. *Earth Surf. Process. Landf.* **2007**, *32*, 165–179.

31. Siart, C.; Bubenzer, O.; Eitel, B. Combining digital elevation data (SRTM/ASTER), high resolution satellite imagery (Quickbird) and GIS for geomorphological mapping: A multi-component case study on Mediterranean karst in Central Crete. *Geomorphology* **2009**, *112*, 106–121. [[CrossRef](#)]
32. Xu, M.; Wang, D.; Qi, J. Study on morphological characteristics of karst landform based on the fractal theory. *J. Chengdu Univ. Technol.* **2011**, *38*, 328–333.
33. Liang, F.; Xu, B. Discrimination of tower-, cockpit-, and non-karst landforms in Guilin, Southern China, based on morphometric characteristics. *Geomorphology* **2014**, *204*, 42–48. [[CrossRef](#)]
34. Huang, W.; Deng, C.; Day, M.J. Differentiating tower karst (fenglin) and cockpit karst (fengcong) using DEM contour, slope, and centroid. *Environ. Earth Sci.* **2014**, *72*, 407–416. [[CrossRef](#)]
35. Purkis, S.; Rowlands, G.; Riegl, B.; Renaud, P. The paradox of tropical karst morphology in the coral reefs of the arid Middle East. *Geology* **2010**, *38*, 227–230. [[CrossRef](#)]
36. Kakavas, M.; Nikolakopoulos, K.G.; Kyriou, A.; Zagana, H. Assessment of freely available DSMs for automatic karst feature detection. *Arab. J. Geosci.* **2018**, *11*, 388. [[CrossRef](#)]
37. Rajabi, A. *Sinkhole Detection and Quantification Using LiDAR Data*; University of Central Florida: Orlando, FL, USA, 2018.
38. Sweeting, M.M. *Karst in China: Its Geomorphology and Environment*; Springer: Berlin, Germany, 1995.
39. Ford, D.; Williams, P. *Karst Hydrogeology and Geomorphology*; Wiley: Hoboken, NJ, USA, 2007.
40. Deng, Z.; Lin, Y.; Zhang, M.; Liu, G.; Wei, Z. *Karst and Geological Structure in Guilin*; Chongqing Publishing House: Chongqing, China, 1988.
41. Zhu, X. *Guilin Karst*; Shanghai Scientific and Technical Publishers: Shanghai, China, 1988.
42. Daoxian, Y.; Drogue, C.; Aide, D.; Wenke, L.; Wutian, C.; Bidaux, P.; Razack, M. Hydrology of the Karst aquifer at the experimental site of Guilin in southern China. *J. Hydrol.* **1990**, *115*, 285–296. [[CrossRef](#)]
43. Xiong, L.; Tang, G. *Loess Landform Inheritance: Modeling and Discovery*; Springer: Singapore, 2019.
44. Wu, Q.; Deng, C.; Chen, Z. Automated delineation of karst sinkholes from LiDAR-derived digital elevation models. *Geomorphology* **2016**, *266*, 1–10. [[CrossRef](#)]
45. Oksanen, J.; Sarjakoski, T. Error propagation of DEM-based surface derivatives. *Comput. Geosci.* **2005**, *31*, 1015–1027. [[CrossRef](#)]
46. Oksanen, J.; Sarjakoski, T. Uncovering the statistical and spatial characteristics of fine toposcale DEM error. *Int. J. Geogr. Inf. Sci.* **2006**, *20*, 345–369. [[CrossRef](#)]
47. Podobnikar, T.; Vrečko, A. Digital Elevation Model from the Best Results of Different Filtering of a LiDAR Point Cloud. *Trans. GIS* **2012**, *16*, 603–617. [[CrossRef](#)]
48. Podobnikar, T.; Székely, B. Towards the automated geomorphometric extraction of talus slopes in Martian landscapes. *Planet. Space Sci.* **2015**, *105*, 148–158. [[CrossRef](#)]
49. Tang, G. Progress of DEM and digital terrain analysis in China. *Acta Geographica Sinica.* **2014**, *69*, 1305–1325.
50. Toulia, E.; Kokinou, E.; Panagiotakis, C. The contribution of pattern recognition techniques in geomorphology and geology: The case study of Tinos Island (Cyclades, Aegean, Greece). *Eur. J. Remote Sens.* **2018**, *51*, 88–99. [[CrossRef](#)]
51. Verbovšek, T.; Gabor, L. Morphometric properties of dolines in Matarsko podolje, SW Slovenia. *Environ. Earth Sci.* **2019**, *78*, 396. [[CrossRef](#)]
52. Tarboton, D.G.; Bras, R.L.; Rodriguez-Iturbe, I.; Rodríguez-Iturbe, I. On the extraction of channel networks from digital elevation data. *Hydrol. Process.* **1991**, *5*, 81–100. [[CrossRef](#)]
53. Sagar, B.S.D.; Murthy, M.B.R.; Rao, C.B.; Raj, B. Morphological approach to extract ridge and valley connectivity networks from Digital Elevation Models. *Int. J. Remote Sens.* **2003**, *24*, 573–581. [[CrossRef](#)]
54. Koka, S.; Anada, K.; Nomaki, K.; Sugita, K.; Tsuchida, K.; Yaku, T. Ridge Detection with the Steepest Ascent Method. *Procedia Comput. Sci.* **2011**, *4*, 216–221. [[CrossRef](#)]
55. Burrough, P.A.; McDonnell, R.A.; Lloyd, C.D. *Principles of Geographical Information Systems*; Oxford University Press: Oxford, UK, 2015.
56. Yang, X.; Tang, G.; Meng, X.; Xiong, L. Saddle Position-Based Method for Extraction of Depressions in Fengcong Areas by Using Digital Elevation Models. *ISPRS Int. J. Geo Inf.* **2018**, *7*, 136. [[CrossRef](#)]
57. Assunção, R.M.; Neves, M.C.; Câmara, G.; Freitas, C.D.C. Efficient regionalization techniques for socio-economic geographical units using minimum spanning trees. *Int. J. Geogr. Inf. Sci.* **2006**, *20*, 797–811. [[CrossRef](#)]
58. Jain, A.K. Data Clustering: 50 Years beyond K-means. *Pattern Recognit. Lett.* **2010**, *31*, 651–666. [[CrossRef](#)]

59. William, B.; Elizabeth, L. Karst geomorphology. *Earth Sci. Rev.* **1983**, *19*, 350–352.
60. Xiong, K. Hydrodynamic genetics of cone karst and tower karst—With special reference to the middle Guizhou. *Carsologica Sin.* **1994**, *3*, 237–246.



© 2019 by the authors. Licensee MDPI, Basel, Switzerland. This article is an open access article distributed under the terms and conditions of the Creative Commons Attribution (CC BY) license (<http://creativecommons.org/licenses/by/4.0/>).